The Electronic Spectrum of Methyleneimine

ARTICLE *in* THE JOURNAL OF PHYSICAL CHEMISTRY A · APRIL 2004

Impact Factor: 2.69 · DOI: 10.1021/jp037938+

3 AUTHORS, INCLUDING:

Paul J Dagdigian
Johns Hopkins University
323 PUBLICATIONS **6,167** CITATIONS

The Electronic Spectrum of Methyleneimine

Alexey Teslja, Boris Nizamov,† and Paul J. Dagdigian*

Department of Chemistry, The Johns Hopkins University, Baltimore, Maryland 21218-2685

Received: December 19, 2003; In Final Form: March 11, 2004

Cavity ring-down spectroscopy (CRDS) has been employed to observe the electronic spectrum of methyleneimine (H_2CNH), which is the simplest imine compound. This species was prepared by the pyrolysis of methyl azide. The CRDS signals over the wavelength range 234 to 260 nm were recorded as a function of the temperature of a heated section of tubing upstream of the CRDS cell. The absorption spectrum of methyleneimine was found to be broad and structureless, with an absorption maximum near 250 nm. The absorption cross section of methyleneimine was estimated by comparison with the absorption spectrum of methyl azide. The 118-nm 1-photon photoionization and the UV multiphoton ionization mass spectra of a molecular beam of unpyrolyzed and pyrolyzed methyl azide were also investigated. The strongest mass peak in the multiphoton ionization of methyleneimine was found to be $m/e = 28$, corresponding to H_2CN^+ or $HNCH^+$. These results are used to interpret the excited electronic states and photochemistry of methyleneimine.

1. Introduction

Methyleneimine (H_2CNH) is the simplest member of the imine family of compounds, which possess a carbon−nitrogen double bond. The imines are very reactive and normally decompose by polymerization, oxidation, or hydrolysis. The transient H_2CNH molecule has been observed in the pyrolysis of methylamine[1,2] and other amines,[3] as well as in the pyrolysis of methyl azide[4,5] and other azido compounds.[6−8] It is also of interest in astrophysics and has been observed in dark interstellar dust clouds.[9,10] Methyleneimine has been identified in the CO_2 laser-assisted decomposition of RDX at 0.1 to 3 atm by Litzinger and co-workers.[11]

Methyleneimine has been investigated with several spectroscopic techniques. Its microwave spectrum has been reported, and a molecular structure for the ground electronic state derived.[1] The infrared absorption spectrum has been investigated by both matrix isolation spectroscopy[12] and in the gas phase.[3] All nine fundamental vibrational transitions have been observed in high-resolution gas-phase experiments using Fourier transform and laser-Stark spectroscopy.[13−16] In most of these studies, H_2CNH was prepared by pyrolysis of methylamine.

The electronic spectrum of methyleneimine has not been previously reported. It would be interesting to observe electronic transitions both to gain experimental information on the excited electronic states of this molecule and to develop a diagnostic based on electronic spectroscopy for the detection of methyleneimine, e.g., for studies of its reaction kinetics. The use of methylamine as a precursor, employed in the microwave and infrared studies mentioned above, is not so convenient since methylamine absorbs[17] in the spectral region where methyleneimine may be expected to absorb.

An isomer of methyleneimine is methylnitrene, CH_3N, which is related to the prototype nitrene, imidogen (NH), by methyl substitution. In analogy with the electronic structure of NH, the ground $\tilde{X}^3A_2$ electronic state of CH_3N has triplet spin multiplicity, with a C_{3v} equilibrium structure. The electronic spectrum of CH_3N was reported by Carrick et al.,[18] and the $\tilde{A}^3E-\tilde{X}^3A_2$ transition was assigned,[19] analogous to the well-known NH $A^3\Pi-X^3\Sigma^-$ transition. Methylnitrene, prepared by the interaction of metastable molecular nitrogen and methyl azide, has also been trapped in solid nitrogen at 10 K and studied spectroscopically.[20]

In contrast to the stability of CH_3N on the lowest triplet potential energy surface (PES), CH_3N rearranges through a 1,2-hydrogen shift to the methyleneimine isomer on the lowest singlet PES. This rearrangement occurs so rapidly that chemical trapping and even detection by femtosecond flash photolysis[21] have failed. The photodetachment spectrum of the CH_3N^- anion shows[22] transitions to vibrational levels of neutral CH_3N in both the ground $\tilde{X}^3A_2$ and singlet excited $\tilde{a}^1E$ state, which is the analogue of the metastable NH($a^1\Delta$) state. The $\tilde{a}^1E$ state thus survives long enough to be visible in the photoelectron kinetic energy distribution. The ν_6 vibrational mode was not observed for the $\tilde{a}^1E$ state. This mode is thought to be the vibrational degree of freedom enabling the rearrangement to methyleneimine. The isomerization of CH_3N has been investigated theoretically.[23−26] Recent quantum chemical calculations[27] show that singlet CH_3N is a real energy minimum, with an estimated barrier to rearrangement of 10 ± 4 kJ mol^{-1}. Hence, the bands observed in photodetachment spectroscopy reflect a real minimum, and not a transition state.

The pyrolysis of azides has been investigated by photoelectron spectroscopy.[4,5] This process proceeds on the singlet PES and yields the imine, rather than the nitrene. In the case of the pyrolysis of methyl azide, the identity of the methyleneimine product was confirmed by comparison of the photoelectron spectrum with that from the pyrolysis of another precursor, *N*-chloromethylamine,[5] as well as from the pyrolysis of methylamine.[2] Pyrolysis of methyl azide initially yields H_2CNH and N_2 at ∼850 K. At higher temperatures, H_2CNH further decomposes to yield HCN. Other pyrolytic precursors have been found to yield methyleneimine, e.g., 2-azidoacetic acid,[6] azidoacetone,[7] and 2-azidoethanol.[8] Methyl azide is a convenient pyrolytic precursor for the study of the electronic spectrum of methyleneimine. The absorption spectrum of methyl azide has a weak absorbance maximum at 286 nm and a strong peak at 215 nm,[28] and absorption by methyl azide should cause much less interference than methylamine precursor for the observation

* Corresponding author. Paul J. Dagdigian. Telephone: 410-516-7438. Fax: 410-516-8420. E-mail: pjdagdigian@jhu.edu.

† Present address: Department of Chemistry, The University of California, Berkeley, CA 94720.

10.1021/jp037938+ CCC: $27.50
Published on Web 04/27/2004

of the electronic spectrum of methyleneimine. Moreover, the temperatures required for the pyrolysis of methyl azide are much lower than for methylamine.

Recently, the photoelectron spectrum of the methylnitrene isomer of H_2CNH, $CH_3N(\tilde{X}^3A_2)$, has been reported in the thermal decomposition of methyl azide.[29] In this case, a mixture of CH_3N_3 and NO was passed through a heated tube filled with a molecular sieve positioned 1−2 cm before the photon interaction region of the spectrometer. Thus, it is likely that CH_3N is produced on the surface of the molecular sieve, and not in the gas phase. The triplet $CH_3N(\tilde{X}^3A_2)$ radical has also been observed by laser fluorescence excitation in the UV photolysis of methyl azide.[30] It is quite likely that H_2CNH is also formed in the UV photolysis of methyl azide, but this pathway has not been directly observed.

The competition between decomposition of methyl azide on the ground singlet PES to yield the imine and intersystem crossing to the lowest triplet PES has been investigated computationally.[24] The activation barrier for the spin-allowed and spin-forbidden pathways are similar. In the unimolecular decomposition of selected vibrational levels of the related HN_3 molecule,[31,32] fragmentation on the singlet PES to yield $NH(a^1\Delta) + N_2$ fragments dominated over spin-forbidden decay to form $NH(X^3\Sigma^-)$ when both channels were energetically accessible.

There has been some theoretical work to characterize the electronic states of H_2CNH.[33−37] The ground electronic state has a planar equilibrium geometry.[1] As in the isoelectronic ethylene molecule,[38−40] the S_1 and T_1 states are computed to have a nonplanar equilibrium geometry, with a dihedral angle of 90° between the planes containing the CH_2 and CNH moieties.[33,35] The vertical excitation energy of the S_1 state [estimated to be 5.44 and 4.98 eV (refs 34 and 35, respectively)] is thus expected to be greater than the excitation energy to the zero-point level of the excited state, and the Franck−Condon principle dictates that the $S_1 \leftarrow S_0$ transition should be spread over a broad wavelength range.

The dependence of the electronic energies of the S_0, S_1, and T_1 states of H_2CNH upon the dihedral angle between the two halves of the molecule has been investigated theoretically.[33] A conical intersection between S_1 and S_0 is found near the geometry of the minimum energy of the S_1 state. This crossing will lead to internal conversion in the molecule, and the internal energy thus available in the S_0 state will be sufficient to allow fragmentation of the molecule, as we discuss below.

In this paper, we report a combined cavity ring-down spectroscopy (CRDS) and laser ionization study of the electronic spectrum of methyleneimine using methyl azide as a pyrolytic precursor. The CRDS technique[41,42] has shown great utility for the spectroscopic study and detection of polyatomic transient intermediates whose excited electronic states do not decay radiatively. In our laboratory, we have previously employed CRDS for a study of the H_2CN radical.[43] In the present study, we follow the pyrolysis of methyl azide by both CRDS and 1-photon photoionization mass spectrometry. We present the first report of the electronic absorption spectrum of methyleneimine and provide an estimate of its absorption cross section through comparison with the spectrum of methyl azide. We have also investigated the multiphoton ionization of pyrolyzed methyl azide.

2. Experimental Section

Two types of experiments were carried out to investigate methyleneimine formed in the pyrolysis of methyl azide, namely CRDS and laser ionization experiments. The experimental arrangement employed for each is described below in turn. Methyl azide (CH_3N_3) was prepared by reacting dimethyl sulfate with sodium azide (both obtained from Aldrich).[5] Sodium azide (0.1 mol) was dissolved (10%) in water, and the solution was heated to about 80 °C. Sodium hydroxide was added to bring the pH above 8. Next, dimethyl sulfate (0.1 mol) was added to the reaction mixture. Approximately 4 mL of methyl azide distillate was collected in a receiving flask held at dry ice temperature. The methyl azide product was stored in a closed vessel kept at dry ice temperature. Deuterated methyl azide (CD_3N_3) was prepared in a similar manner, with d_6-dimethyl sulfate as the methylating reagent.

The CRDS experiments were carried out in a flow apparatus. Methyl azide, diluted in argon, was passed through 1.30-cm diameter quartz tubing and heated in a 5-cm long section located in different runs 10 to 90 cm from the cavity ring-down (CRD) cell. The flow from the quartz tubing (estimated flow speed of 10 cm/s) entered the center of the CRD cell and was evacuated from both ends of a 32-cm long central section (2.5-cm diam) of the cell. The CRD mirrors (Research Electro Optics, Boulder, CO; 99.6% reflectivity at 238 nm, estimated by the CRD photon decay lifetime) were mounted on the ends of 17-cm long arms (3.8-cm diameter) attached to the central section. The total length of the CRD cell was thus 66 cm. A small flow of argon was directed at the mirrors to minimize reduction of their reflectivity from the methyl azide pyrolysis products. The temperature of the heated section of quartz tubing was measured with a chromel−alumel thermocouple referenced to an ice−water bath.

The frequency-doubled output from a tripled Nd:YAG (Continuum Surelite I)-pumped dye laser (Lambda Physik FL3002E) was injected into the CRD cell through one of the mirrors. The second harmonic was separated from the fundamental dye laser radiation by a set of four Pellin-Broca prisms. The temporal width of a laser pulse was ∼5 ns, and the spectral bandwidth of the doubled UV output was 0.4 cm^{-1}. Typical UV pulse energies were 0.1−0.5 mJ. An aperture was employed to control the size of the UV laser beam in order to reduce the number of transverse modes excited in the cavity. The CRD signal was detected through the rear mirror with a Hamamatsu R282 photomultiplier tube (PMT). A diffuser was placed in front of the PMT to minimize possible problems arising from the nonuniformity of the PMT area response.

The CRD signal was detected with a LeCroy LT372 digital oscilloscope. The signal from each shot was transferred through a GPIB connection to a computer, and a weighted linear least-squares fit of the logarithm of the signal as a function of time was employed to compute the photon decay lifetime from each laser shot. The typical decay lifetime for the empty cavity was 500 ns at 240 nm. Empty-cavity lifetimes of >300 ns were observed for wavelengths as long as 258 nm. At a given wavelength, single-shot decay lifetimes τ were averaged over a preset number of shots (10−30), and then the dye laser wavelength was stepped to the next wavelength point. Ring-down lifetimes could be determined to an accuracy of 1.5% in a 10-shot average.

Scans were typically taken over a wide wavelength range, for which the reflectivity of the CRD mirrors could vary significantly. This led to large changes in the detected PMT signal, and consequently distortions in the decay waveforms were observed for large PMT signal amplitudes. Our data acquisition program was subsequently modified to allow for the variation of the PMT voltage through an externally programmable high-voltage power supply, to maintain a constant PMT output peak amplitude over a scan.

To determine the absorbance α (product of the molecular number density N and absorption cross section σ), the photon

decay rate (reciprocals of the lifetimes) at a given wavelength was subtracted from the corresponding empty-cavity decay rate. We compute the absorbance as follows:

$$\alpha = c^{-1}(\tau^{-1} - \tau_0^{-1})\,(L/l) \qquad (1)$$

where c is the speed of light, L is the length of the CRD cavity, and l is the length of the central portion of the cavity, in which the absorber is present. The empty-cavity lifetime τ_0 (argon only flowing through the CRD cell) was recorded over the scanned wavelength range both before and after a series of CRD absorption spectra were recorded.

The apparatus in which the laser ionization experiments were carried out has been described in detail previously.[44,45] Methyleneimine was prepared in a supersonic beam by flash pyrolysis[46,47] of a dilute mixture (5−8% mole fraction) of methyl azide in argon (total pressure < 800 Torr) by passage through a resistively heated SiC tube (0.5 mm ID, 2 mm OD) attached to a pulsed solenoid valve (General Valve). The free-jet beam was introduced into the ionization region of a time-of-flight mass spectrometer (TOFMS).[48] To follow the pyrolysis of methyl azide, 1-photon photoionization at 118 nm was employed. Radiation at 118 nm was generated by frequency tripling Nd:YAG 355-nm radiation in a Xe cell (25 Torr pressure, 33 cm long). The 355-nm frequency-tripled output of a Nd:YAG laser was focused into the cell with a 25-cm focal length quartz lens, and a 6.3-cm focal length MgF_2 lens softly focused the generated 118-nm light into the ionization region of the TOFMS. The 355-nm pulse energy was kept at ∼3.5 mJ or below in order to avoid multiphoton ionization involving a combination of 118- and 355-nm photons.

The same apparatus was employed to investigate resonance-enhanced multiphoton ionization (REMPI) of methyleneimine. In this case, frequency-doubled laser radiation from the Nd:YAG laser-pumped dye laser employed in the CRD experiments was focused into the ionization region of the TOFMS with a 25-cm focal length lens. Typical UV pulse energies were 0.1−0.5 mJ. This energy was kept low in order to minimize the photolytic destruction of methyl azide.

3. Results

3.1. CRDS Experiments. Figure 1 shows the evolution of the cavity ring-down absorption spectrum within the 234−244 nm wavelength range of a flow of methyl azide diluted in argon as the temperature of a heated section upstream of the CRD cell is raised. Spectrum (a) is that of methyl azide, which has a weak absorbance maximum at 286 nm (maximum absorption cross section 5.5×10^{-20} cm^2) and a strong peak at 215 nm (maximum absorption cross section 1.64×10^{-18} cm^2).[28] The absorption spectrum of methyl azide matches well with the wavelength dependence of spectrum (a).

As the temperature of the heated section of quartz tubing upstream of the CRD cell is raised, the absorbance at long wavelengths increases, as illustrated by scans (b)−(e) in Figure 1. There also appears to be an isosbestic point near 234 nm. Essentially identical spectra as a function of the temperature of the heated section were recorded with the heated section at distances of 10 to 90 cm from the CRD cell. This suggests that methyleneimine is not being lost to a significant degree during the flow from the heated section to the CRD cell.

CRD spectral scans were recorded in two additional wavelength ranges to the red of that displayed in Figure 1. Figure 2 presents the recorded cavity ring-down absorption spectrum for the 240−256 nm wavelength range of a flow of methyl azide diluted in argon as the temperature of a heated section upstream of the CRD cell is raised. We see from scan (a) in Figure 2 that the absorption spectrum of methyl azide reaches a minimum in this wavelength range between the two previously quoted absorption maxima of methyl azide. We see that the recorded absorbance in this wavelength range grows as the temperature of the heated section of tubing is raised. This absorbance has a maximum at a wavelength near 249 nm. We found that the temperature-induced changes in absorbance depended somewhat upon the experimental conditions related to the residence time in the heated section (pressure, length of heated region, etc.). The efficiency of the pyrolysis was greater at lower pressure. In comparing spectra taken in different wavelength regions, we employed spectra taken under the same conditions.

Figure 3 plots the measured absorbance at 250.0 nm as a function of the temperature of the heated section of tubing. It can be seen that the absorbance decreases slightly as a function

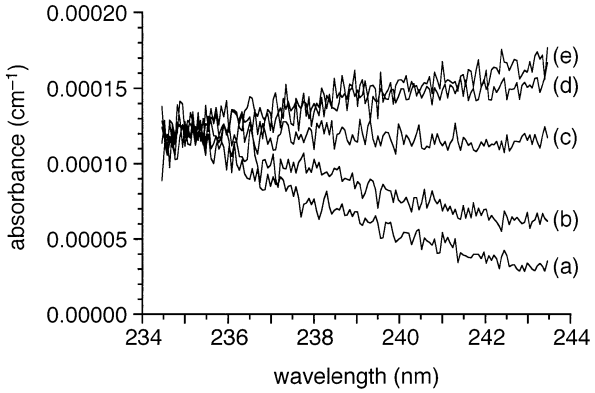

Figure 1. Room-temperature CRD absorption spectrum in the 234−244 nm spectral range of a flow of methyl azide diluted in argon (total pressure 0.45 Torr) which was passed through a section of quartz tubing located 16 cm from the cavity ring-down cell and heated to (a) room temperature, (b) 650 K, (c) 730 K, (d) 810 K, and (e) 900 K. The absorbances were computed as the average over 10 laser shots. Spectrum (a) represents the spectrum of methyl azide, while spectra (b)−(e) show an increasing contribution due to absorption of the H_2-CNH pyrolysis product. On the basis of the known (ref 28) absorption cross section of methyl azide, the room-temperature absorbance corresponds to a methyl azide partial pressure of 0.018 Torr.

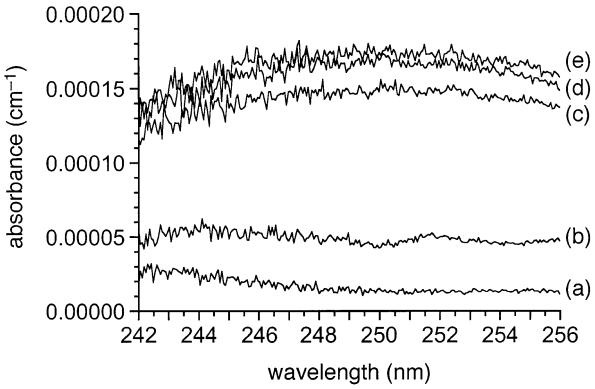

Figure 2. Room-temperature CRD absorption spectrum in the 241−256 nm spectral range of a flow of methyl azide diluted in argon (total pressure 0.41 Torr) which was passed through a section of quartz tubing located 16 cm from the cavity ring-down cell and heated to (a) room temperature, (b) 670 K, (c) 830 K, (d) 870 K, and (e) 960 K. The absorbances were computed as the average over 10 laser shots. Spectrum (a) represents the spectrum of methyl azide, while spectra (b)−(f) show an increasing contribution due to absorption of the H_2-CNH pyrolysis product. On the basis of the known (ref 28) absorption cross section of methyl azide, the room-temperature absorbance corresponds to a methyl azide partial pressure of 0.0165 Torr.

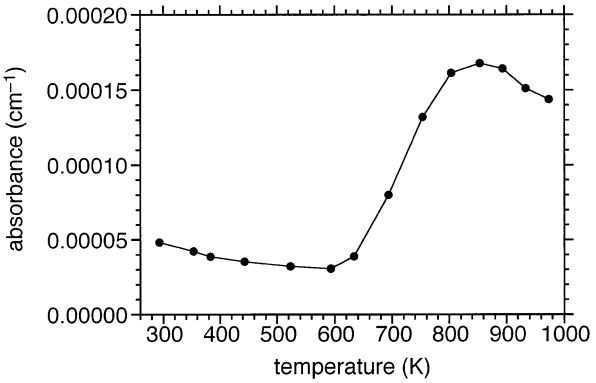

Figure 3. Absorbance at 250.0 nm of a flow of methyl azide diluted in argon (total pressure 0.72 Torr) as a function of the temperature of a heated section of quartz tubing located 16 cm from the cavity ring-down cell. On the basis of the known (ref 28) absorption cross section of methyl azide, the room-temperature absorbance corresponds to a methyl azide partial pressure of 0.060 Torr.

of temperature until ~600 K. This reduction can be explained by the slight decrease in the gas density for constant pressure as a function of temperature. Above 600 K, the absorbance rises rapidly and reaches a maximum value by ~860 K. This is the same temperature range over which the pyrolysis of methyl azide was observed[5] through photoelectron spectroscopy to yield the methyleneimine molecule. A slight decrease in the absorbance is observed for temperatures slightly above 860 K, and the absorbance starts to decrease somewhat faster for temperatures above 900 K, up to 970 K, the highest temperature investigated here. We did not raise the temperature of the heated section up to temperatures at which methyleneimine was observed[4,5] by photoelectron spectroscopy to decompose completely to HCN and H_2. It can be seen that the absorbance change at 250 nm displayed in Figure 3 is somewhat less than that discernible from the spectra plotted in Figure 2. This reflects differences in the efficiency of the pyrolysis due to the differing flow conditions.

The observed range of excitation energies for the pyrolysis product of methyl azide is similar to that calculated[33,35] for the transition to the S_1 state of methyleneimine. The previously quoted[34,35] vertical excitation energies correspond to wavelengths of 228 and 250 nm. From the observed temperature at which the new absorption is seen and the wavelength of the observed absorption maximum, we assign the molecular carrier of this newly observed UV absorption spectrum as methyleneimine. Our observation of an isosbestic point near 234 nm and the absence of a loss in the strength of the absorbance when the distance of the heated section of tubing was varied both imply that, under the conditions of our experiment, methyl azide is essentially quantitatively converted to methyleneimine and that the loss of methyleneimine on the walls and within the tubing before the cell is not significant.

The spectra displayed in Figures 1 and 2 do not show any resolvable structure above the noise of the plotted spectra. CRD scans were also taken in selected wavelength ranges with small wavelength increments and the CRD lifetimes computed from more averaged laser shots per point. In no case, did we observe any structure on the absorption spectrum of methyleneimine.

To derive the absorption spectrum of pure methyleneimine from spectra of partially photolyzed methyl azide, such as those displayed in Figures 1 and 2, a least-squares fitting procedure was employed. At a given wavelength and heater temperature, the absorbance $\alpha(\lambda, T)$ can be expressed in terms of the absorption cross sections σ of methyl azide and methyleneimine

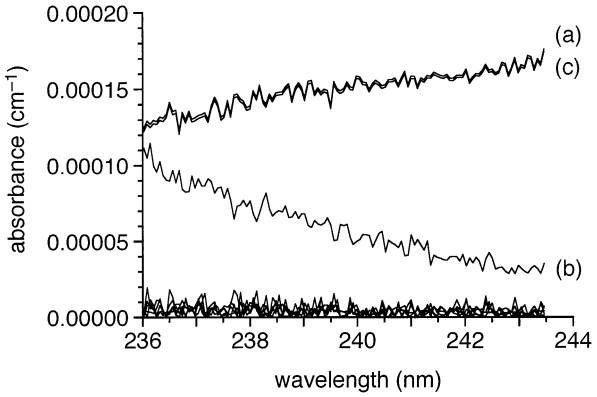

Figure 4. Room-temperature CRD absorption spectrum of methyleneimine in the 236−244 nm spectral range, determined by a least-squares fit of the spectra displayed in Figure 1 to eq 2. (a) Derived spectrum for methyleneimine; (b) spectrum of methyl azide [Figure 1(a)]; (c) spectrum recorded at 900 K [Figure 1(e)]. For clarity, plots of scans (a) and (c) from Figure 1 are displayed in this figure. The plots just above the *x*-axis are the residuals of the fits to all the spectra in Figure 1.

as

$$\alpha(\lambda, T) = N(CH_3N_3, T)\,\sigma(CH_3N_3, \lambda) + N(H_2CNH, T)\,\sigma(H_2CNH, \lambda) \quad (2)$$

where N(molecule, T) is the number density of the given species at temperature T. We can ignore absorption due to other fragmentation products such as N_2, HCN, and H_2 since these species do not absorb in the wavelength investigated in this study.

Spectra were recorded at a series of temperatures $\{T_i$, where $i = 1$ to $m\}$, each over the same grid of wavelengths $\{\lambda_j$, where $j = 1$ to $n\}$. In addition, a spectrum with the heater off was also recorded under identical conditions; this provides us with a spectrum of undecomposed methyl azide. We treat the concentrations $N(CH_3N_3, T_i)$ and $N(H_2CNH, T_i)$ at each temperature and the spectrum of methyleneimine on the above grid of wavelengths, $\{\sigma(H_2CNH, \lambda_j)$, where $j = 1$ to $n\}$, as parameters to be fit, yielding a total of $2m + n$ variables. From eq 2, we see that our fit is a nonlinear least-squares fitting problem because the product of the concentration and absorption cross section of methyleneimine appears in this equation. We have employed the Levenberg−Marquardt nonlinear fitting procedure[49] to determine these parameters, and hence to obtain the absorption spectrum of methyleneimine.

We have applied this fitting procedure to the spectra displayed in Figure 1. The spectra were truncated on the blue end at 236 nm because of the large noise in the recorded CRD spectra for wavelengths < 236 nm. Scan (a) in Figure 4 presents the derived absorption spectrum for methylenemine. For comparison, spectra for methyl azide [scan (b)] and the spectrum recorded with the heated section at the highest temperature (900 K) [scan (c)] are also displayed in Figure 4. It can be seen that the derived spectrum for methylenemine is very close to that of scan (c) and suggests that at 900 K methyl azide has been essentially completely pyrolyzed to methylenemine. Indeed, the fitted value for $N(H_2CNH, T = 900$ K) is 0.99 (with normalization of the number densities so that $N(CH_3N_3, T)$ equals unity at room temperature). With this analysis, we may reasonably take spectra recorded with the heated section at ~900 K as being representative of the spectrum of methylenemine itself.

To determine the absorption spectrum of methylenemine over a wide wavelength range, we have spliced together spectra taken

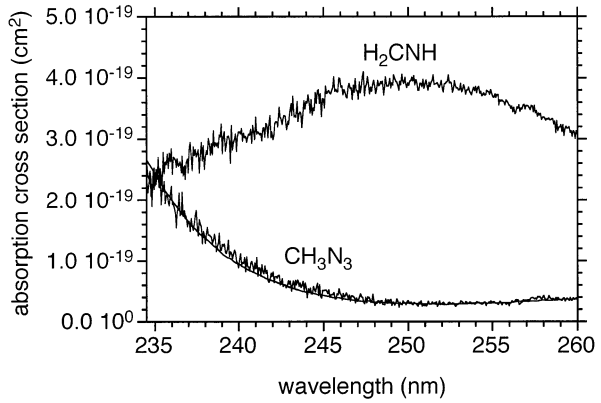

Figure 5. Room-temperature absorption spectra of methyl azide (smooth solid line: measured with a Cary 219 spectrophotometer; noisy line: CRD spectrum) and of methyleneimine, determined by CRDS in this work. The absolute values of the absorption spectra were normalized with the aid of a published absorption spectrum (ref 28).

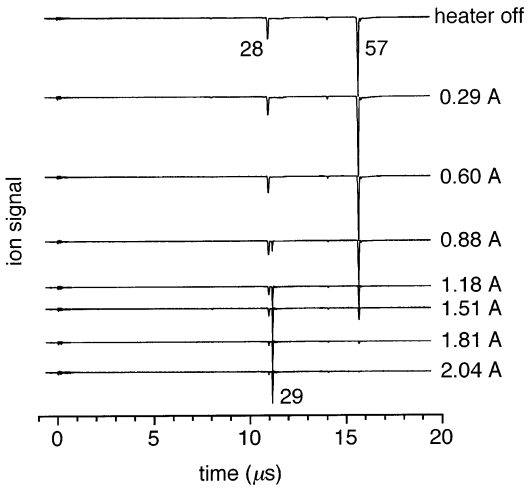

Figure 6. Time-of-flight 118-nm photoionization mass spectrum of a pyrolyzed supersonic beam of methyl azide. Mass spectra are reported as a function of the current through the SiC pyrolysis tube in the molecular beam source.

with three different laser dyes. Since the partial pressure of methyl azide was not the same in all these scans, we have rescaled the spectra in the individual dye laser regions so that the absorption spectrum of methyl azide was continuous and smooth over the entire wavelength region. Figure 5 presents the absorption spectra of both methyl azide and methylenemine over the 234−260 nm wavelength range. These spectra (absorption cross sections) have been put on an absolute scale with the aid of a published[28] absorption spectrum for methyl azide.

We see from Figure 5 that the absorption spectrum of methylenemine peaks at ~249 nm and is quite broad. The absorbance at 249 nm is much larger than for methyl azide at that wavelength, and the maximum absorption cross section for methylenemine is computed to equal approximately 4×10^{-19} cm^2. As discussed above, no structure was discerned in the absorption spectrum.

3.2. Ionization Studies. The adiabatic ionization potentials of methyl azide and methyleneimine are 9.81 ± 0.02 and 9.9 ± 0.2 eV, respectively,[50,51] so that 118 nm photons have sufficient energy (10.49 eV) to ionize both species. Figure 6 displays 118 nm photoionization time-of-flight mass spectra of methyl azide, diluted in argon, as a function of the current passing through the SiC pyrolysis tube in the pyrolysis beam source. The mass spectrum obtained with the source at room temperature

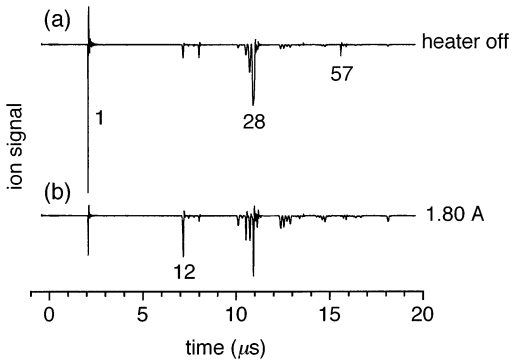

Figure 7. Laser ionization (wavelength 240.0 nm) time-of-flight mass spectra of (a) unpyrolyzed and (b) pyrolyzed CH_3N_3 (heater current 1.80 A). The masses of prominent peaks are identified.

is very similar to the electron-impact mass spectrum of methyl azide,[52] with strong peaks at $m/e = 57$ (parent) and 28. As the temperature of the heated tube in the pyrolysis source is raised, these peaks decrease in intensity, and a $m/e = 29$ ion appears with increasing intensity (see Figure 6). This mass-to-charge ratio corresponds to the parent ion for methyleneimine and is consistent with the assigned[5] initial fragmentation process for the pyrolysis of methyl azide. At the highest pyrolysis source temperature studied, the masses associated with the ionization of parent methyl azide do not appear in the time-of-flight spectrum.

We also investigated the tunable UV multiphoton ionization of methyleneimine. With the adiabatic ionization potential quoted above, we compute that UV wavelengths shorter than 250 nm are required for REMPI through a 1-photon excited electronic state (1 + 1 scheme). This wavelength is at approximately the maximum absorption cross section for the transition in methyleneimine identified in the previous section. For reference, we note that the vertical ionization potential [10.62 ± 0.02 eV (refs 2,4,6)] of methyleneimine is slightly higher than the adiabatic ionization potential.

We have recorded time-of-flight mass spectra with multiphoton ionization using focused UV laser radiation for both CH_3N_3 and CD_3N_3. Figure 7 presents mass spectra of unpyrolyzed [scan (a)] and pyrolyzed [scan (b)] CH_3N_3 at a UV laser wavelength of 240.0 nm. On the basis of our 118-nm photoionization study, methyl azide has been completely pyrolyzed and converted to methyleneimine under the conditions of scan (b). We see in scan (a) that the laser ionization of unpyrolyzed CH_3N_3 precursor yields a weak parent ion mass peak ($m/e = 57$) and strong fragment peaks at $m/e = 28$ and 1. In contrast to 118 nm 1-photon ionization [see Figure 6], the $m/e = 28$ peak is broad, suggesting significant kinetic energy release in the formation of this ion and/or neutral counterpart. The laser ionization mass spectrum of pyrolyzed CH_3N_3 [scan (b)] displays a number of ion masses. We note that the parent ion of methyleneimine is absent in the mass spectrum. While the $m/e = 28$ ion remains strong in the mass spectrum when methyl azide is pyrolyzed, its time-of-arrival profile is much narrower than in scan (a). Under the conditions of scan (b), this ion arises from the ionization of a methyl azide decomposition product, i.e. methyleneimine. Slightly broad $m/e = 26$ and 27 time-of-arrival profiles are also observed for the laser ionization of unpyrolyzed CH_3N_3, and these peaks are narrower with pyrolyzed CH_3N_3 precursor.

We show in Figure 8 time-of-flight mass spectra for unpyrolyzed [scan (a)] and pyrolyzed [scan (b)] CD_3N_3 at a UV wavelength of 230.8 nm. The laser ionization mass spectrum of the unpyrolyzed CD_3N_3 precursor shows a weak parent ion peak ($m/e = 60$) and a strong peak at $m/e = 30$. The latter ion

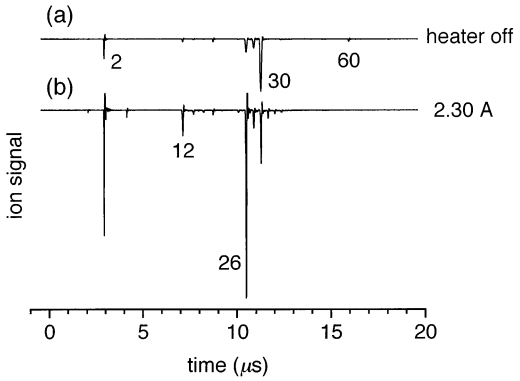

Figure 8. Laser ionization (wavelength 230.0 nm) time-of-flight mass spectra of (a) unpyrolyzed and (b) pyrolyzed CD_3N_3 (heater current 2.30 A). The masses of prominent peaks are identified.

corresponds to $m/e = 28$ for CH_3N_3. Hence, we assign the chemical formulas CH_2N^+ and CD_2N^+ to the $m/e = 28$ and 30 ions, respectively. (There are several isomers possible for ions of these formulas.[53]) Pyrolysis of CD_3N_3 leads to loss of the parent ion signal and a sharpening of the time-of-arrival profile for $m/e = 30$ and similarly for the weaker $m/e = 26$ and 28 ions [see scan (b)]. We do see a small $m/e = 32$ ion in scan (b); this corresponds to the parent ion of CD_2ND. The $m/e = 26$ peak observed in Figures 7 and 8 is likely due to CN^+, which can arise from the photolysis/ionization of CH_2N and CD_2N or their positive ions.

We have taken scans as function of the UV wavelength of the yield of both $m/e = 28$ and 1 ions in the laser ionization of pyrolyzed CH_3N_3. Both these ions are observed over the UV wavelength range 230−260 nm. Their yields as a function of UV wavelength did not show any discernible structure.

We also recorded laser ionization spectra of unpyrolyzed and pyrolyzed methyl azide at longer wavelengths (250−300 nm), where at least a 2 + 1 REMPI scheme would be required for the ionization of methyleneimine. Again, the ion observed with the greatest intensity was $m/e = 28$, and no $m/e = 29$ ions were observed in the laser ionization of pyrolyzed CH_3N_3.

From this UV laser ionization study of pyrolyzed methyl azide, we conclude that the parent ion of methyleneimine is not formed to any appreciable extent in the UV multiphoton ionization of methyleneimine. In the next section, we discuss the implications of this observation for the photochemistry of methyleneimine.

4. Discussion

In this paper, we have reported the first observation of the electronic absorption spectrum of methyleneimine, which was generated by pyrolysis of methyl azide and spectroscopically detected by CRDS. By comparison of the absorbances of unpyrolyzed and pyrolyzed methyl azide and with the help of measured[28] absorption cross sections for methyl azide, we have moreover been able to put the absorption spectrum of methyleneimine on an absolute scale.

Figure 5 shows the electronic transition to the S_1 excited state of methyleneimine to be broad and structureless. The broad width of the transition is consistent with the Franck−Condon principle and the very different equilibrium geometries[1,33,35] of the S_0 and S_1 states. The absorption spectrum of the isoelectronic ethylene molecule[38] shows similarly broad electronic transitions to the T_1 (very weak) and S_1 (strong) excited states. As mentioned in the Introduction,[38−40] electronic excitation in ethylene causes a large change in geometry, as the S_0 state has a planar D_{2h} structure, while the T_1 and S_1 excited states favor a nonplanar D_{2d} geometry in which the dihedral angle between the two CH_2 moieties is 90°. Superimposed on the broad ethylene absorptions are poorly resolved features which have the appearance of vibrational progressions. Several different explanations, including progressions in the C−C stretch and torsion vibrational modes, have been put forward to explain this vibrational structure.[54] In contrast to ethylene, we see no hint of vibrational structure on the room-temperature absorption spectrum of methyleneimine. The excited states and absorption spectrum of ethylene are complicated by Rydberg-valence mixing.[38−40] Vertical excitation energies of low-lying Rydberg states have been computed[34] for methyleneimine. Rydberg-valence mixing appears to be much less of an issue in the case of methylenemine since the excitation energy for the S_1 state is significantly less in methyleneimine than in ethylene, while their ionization potentials are similar.[50,51]

As discussed in the Introduction, the S_1 state of methyleneimine likely undergoes facile internal conversion to the ground S_0 state. This leaves the molecule in the ground electronic state with approximately 490 kJ mol^{-1} internal energy. This energy is sufficient to allow several fragmentation pathways to occur. Nguyen et al.[25] have considered the possible pathways, and their energetics and transition states. The possible fragmentation pathways include

$$H_2CNH \rightarrow HCN + H_2, \quad \Delta E = 24.7 \text{ kJ mol}^{-1} \qquad (3a)$$

$$\rightarrow HNC + H_2, \quad \Delta E = 86.2 \text{ kJ mol}^{-1} \qquad (3b)$$

$$\rightarrow H_2CN + H, \quad \Delta E = 347.3 \text{ kJ mol}^{-1} \qquad (3c)$$

$$\rightarrow HCNH + H, \quad \Delta E = 386.6 \text{ kJ mol}^{-1} \qquad (3d)$$

The energies ΔE required for dissociation were obtained from QCISD(T) quantum chemical calculations by Nguyen et al.[25] The energies ΔE_{TS} of the transition states relative to that of the ground vibrational level of H_2CNH lie significantly higher in energy than the dissociation energies for some of these pathways. Values of $\Delta E_{TS} = 407.1$ and 366.1 kJ mol^{-1} were computed[25] for pathways (3a) and (3b), respectively, which both lead to formation of H_2. No activation barrier was reported for pathway (3c), while no low-energy pathway was found for pathway (3d). Sumathi[35] considered pathway (3d) and reported a reaction path from the T_1 state, but not from S_0.

From the computational results presented above, we see that the energy available from excitation of H_2CNH to the S_1 electronic state is sufficient to allow fragmentation to yield both H_2 and H fragments through pathways (3a), (3b), and/or (3c). We have indirect evidence from our UV laser ionization experiments for dissociative decay of electronically excited methyleneimine. In contrast to 118-nm 1-photon photoionization, no parent ions were observed in UV multiphoton ionization of methyleneimine, while for the deuterated isotopomer the parent ion was observed weakly. In place of the parent ion, the ion involving the loss of a hydrogen (or deuterium) atom was observed strongly. The appearance of this fragment ion can be explained by dissociation of electronically excited methyleneimine at the 1-photon level, and subsequent ionization of the H_2CN fragment.

The differing initial kinetic energies of the $m/e = 28$ ions from the UV multiphoton ionization of methyl azide and of methyleneimine can be rationalized from the known energetics and kinematics. If we assume that fragmentation occurs in the

230-nm excitation of methyleneimine at the 1-photon level following pathway (3c), then approximately 1.8 eV of energy will be available to the products. This implies that the mass-28 fragment will have a recoil velocity of 6.5×10^4 cm/s if all of the available energy appears as translational energy of the fragments. This velocity is comparable to the initial laboratory velocity in the molecular beam and would not be expected to lead to a broadening of the $m/e = 28$ ion time-of-arrival profile, as observed. By contrast, the dissociation of 1-photon excited methyl azide will lead to large fragment velocities. The energy of the $H_2CNH + N_2$ fragments is computed[25] to be 230 kJ mol^{-1} lower than that of the methyl azide parent molecule. With the assumption that all the available energy appears as translational energy, this implies that the H_2CNH fragment will have a recoil velocity of 5.1×10^5 cm/s. Even with loss of a hydrogen atom from this fragment, the velocity imparted to a $m/e = 28$ fragment ion from the dissociation of the methyl azide parent will be substantial. This provides an explanation for our observation of a broad $m/e = 28$ time-of-arrival profile in the UV multiphoton ionization of methyl azide.

The present study was initiated to develop a spectroscopic probe for the methyleneimine molecule which would be suitable in studies of the reaction kinetics of this species. CRDS employing the presently observed electronic transition is a suitable method for the determination of methyleneimine concentrations. Laser photolysis of methyl azide[28] should be a convenient source of methyleneimine. One criterion for the use of a photolytic precursor in kinetic studies is that the absorption of the precursor be negligible at the wavelength at which the reactive species is detected. We see from the absorption cross sections presented in Figure 5 that the absorbance of methyleneimine near 250 nm is only an order of magnitude larger than that of methyl azide. This difference in absorbances is probably not sufficient to allow the detection of methyleneimine without interference due to unphotolyzed methyl azide. Methyl isocyanate, which has a significantly smaller absorption cross section[55] at 250 nm than methyl azide but a comparable absorption cross section at 193 nm, may be a more suitable photolytic source of methyleneimine for kinetic studies.

Acknowledgment. This work was supported by the U.S. Army Research Office, under Grant DAAD19-02-1-0323.

References and Notes

(1) Pearson, R.; Lovas, F. J. *J. Chem. Phys.* **1977**, *66*, 4149−4156.
(2) Peel, J. B.; Willett, G. D. *J. Chem. Soc., Faraday Trans. 2* **1975**, *71*, 1799−1804.
(3) Hamada, Y.; Hashiguchi, K.; Tsuboi, M.; Koga, Y.; Kondo, S. *J. Mol. Spectrosc.* **1984**, *120*, 70−80.
(4) Bock, H.; Dammel, R. *Angew. Chem., Int. Ed. Engl.* **1987**, *26*, 504−526.
(5) Bock, H.; Dammel, R. *J. Am. Chem. Soc.* **1988**, *110*, 5261−5269.
(6) Dyke, J. M.; Groves, A. P.; Morris, A.; Ogden, J. S.; Dias, A. A.; Oliveira, A. M. S.; Costa, M. L.; Barros, M. T.; Cabral, M. H.; Moutinho, A. M. C. *J. Am. Chem. Soc.* **1997**, *119*, 6883−6887.
(7) Dyke, J. M.; Groves, A. P.; Morris, A.; Ogden, J. S.; Catarino, M. I.; Dias, A. A.; Olivereira, A. M. S.; Costa, M. L.; Barros, M. T.; Cabral, M. H.; Moutinho, A. M. C. *J. Phys. Chem. A* **1999**, *103*, 8239−8245.
(8) Hooper, N.; Beeching, L. J.; J, M. D.; Morris, A.; Ogden, J. S.; Dias, A. A.; Costa, M. L.; Barros, M. T.; Cabral, M. H.; Moutinho, A. M. C. *J. Phys. Chem. A* **2002**, *106*, 9968−9975.
(9) Godfrey, P. D.; Brown, R. D.; Robinson, B. J.; Sinclair, M. W. *Astrophys. Lett.* **1973**, *13*, 119−121.
(10) Dickens, J. E.; Irvine, W. M.; DeVries, C. H.; Ohishi, M. *Astrophys. J.* **1997**, *479*, 307−312.
(11) Lee, Y.; Tang, C.-J.; Litzinger, T. A. *Combust. Flame* **1999**, *117*, 600−628.
(12) Jacox, M. E.; Milligan, D. E. *J. Mol. Spectrosc.* **1975**, *56*, 333−336.
(13) Duxbury, G.; Kato, H.; Le Lerre, M. L. *Discuss. Faraday Soc.* **1981**, *71*, 97−110.
(14) Halonen, L.; Duxbury, G. *Chem. Phys. Lett.* **1985**, *118*, 246−251.
(15) Halonen, L.; Duxbury, G. *J. Chem. Phys.* **1985**, *83*, 2078−2090.
(16) Halonen, L.; Duxbury, G. *J. Chem. Phys.* **1985**, *83*, 2091−2096.
(17) Baek, S. J.; Choi, K.-W.; Choi, Y. S.; Kim, S. K. *J. Chem. Phys.* **2002**, *118*, 11026−11039.
(18) Carrick, P. G.; Brazier, C. R.; Bernath, P. F.; Engelking, P. C. *J. Am. Chem. Soc.* **1987**, *109*, 5100−5102.
(19) Brazier, C. R.; Carrick, P. G.; Bernath, P. F. *J. Chem. Phys.* **1992**, *96*, 919−926.
(20) Ferrante, R. F. *J. Chem. Phys.* **1987**, *86*, 25−32.
(21) Glownia, J. J.; Misewich, J.; Sorokin, P. P. In *Supercontinuum Sources*; Alfano, R. R., Ed.; Springer: New York, 1989; p 337.
(22) Travers, M. J.; Cowles, D. C.; Clifford, E. P.; Ellison, G. B.; Engelking, P. C. *J. Chem. Phys.* **1999**, *111*, 5349−5360.
(23) Richards, C. J.; Meredith, C.; Kim, S.-J.; Quelch, G. E.; Schaefer, H. F. *J. Chem. Phys.* **1994**, *100*, 481−489.
(24) Arenas, J. F.; Marcos, J. J.; Otero, J. C.; Sanchez-Galvez, A.; Soto, J. *J. Chem. Phys.* **1999**, *111*, 551−561.
(25) Nguyen, M. T.; Sengupta, D.; Ha, T.-K. *J. Phys. Chem.* **1996**, *100*, 6499−6503.
(26) Arenas, J. F.; Marcos, J. I.; Otero, J. C.; Tocón, I. L.; Soto, J. *Int. J. Quantum Chem.* **2001**, *84*, 241−248.
(27) Kemnitz, C. R.; Ellison, G. B.; Kearney, W. L.; Borden, W. T. *J. Am. Chem. Soc.* **2000**, *122*, 1098−1101.
(28) Getoff, N.; Laupert, R.; Schindler, R. N. *Z. Phys. Chem.* **1970**, *70*, 70−86.
(29) Jing, W.; Zheng, S.; Xinjiang, Z.; Xiaojun, Y.; Maofa, G.; Dianxun, W. *Angew. Chem., Int. Ed.* **2001**, *40*, 3055−3057.
(30) Ying, L.; Xia, Y.; Shang, H.; Zhao, X.; Tang, Y. *J. Chem. Phys.* **1996**, *105*, 5798−5805.
(31) Foy, B. R.; Casassa, M. P.; Stephenson, J. C.; King, D. S. *J. Chem. Phys.* **1990**, *92*, 2782−2789.
(32) Casassa, M. P.; Foy, B. R.; Stephenson, J. C.; King, D. S. *J. Chem. Phys.* **1991**, *94*, 250−261.
(33) Bonacic-Koutecky, V.; Michl, J. *Theor. Chim. Acta* **1985**, *68*, 45−55.
(34) Bruna, P. J.; Krumbach, V.; Peyerimhoff, S. D. *Can. J. Chem.* **1985**, *63*, 1594−1608.
(35) Sumathi, R. *J. Mol. Struct.* **1996**, *364*, 97−106.
(36) De Olivera, G.; Martin, J. M. L.; Silwal, I. K. C.; Liebman, J. F. *J. Comput. Chem.* **2001**, *22*, 1297−1305.
(37) Chestnut, D. B. *J. Comput. Chem.* **2001**, *22*, 1702−1711.
(38) Merer, A. J.; Mulliken, R. S. *Chem. Rev.* **1969**, *69*, 639−656.
(39) Ben-Nun, M.; Martinez, T. J. *Chem. Phys.* **2000**, *259*, 237−248.
(40) Krawczyk, R. P.; Viel, A.; Manthe, U.; Domcke, W. *J. Chem. Phys.* **2003**, *119*, 1397−1411.
(41) Scherer, J. J.; Paul, J. B.; O'Keefe, A.; Saykally, R. J. *Chem. Rev.* **1997**, *97*, 25−51.
(42) Berden, G.; Peeters, R.; Meijer, G. *Int. Rev. Phys. Chem.* **2000**, *19*, 565−607.
(43) Nizamov, B.; Dagdigian, P. J. *J. Phys. Chem. A* **2003**, *107*, 2256−2263.
(44) Lambert, H. M.; Dagdigian, P. J. *Chem. Phys. Lett.* **1997**, *275*, 499−505.
(45) Lambert, H. M.; Dagdigian, P. J. *J. Chem. Phys.* **1998**, *109*, 7810−7820.
(46) Kohn, D. W.; Clauberg, H.; Chen, P. *Rev. Sci. Instrum.* **1992**, *63*, 4003−4005.
(47) Stranges, D.; Stemmler, M.; Yang, X.; Chesko, J. D.; Suits, A. G.; Lee, Y. T. *J. Chem. Phys.* **1998**, *109*, 5372−5382.
(48) Varley, D. F.; Dagdigian, P. J. *J. Phys. Chem.* **1995**, *99*, 9843−9853.
(49) Bevington, P. R. *Data Reduction and Error Analysis for the Physical Sciences*; McGraw-Hill: New York, 1969.
(50) Lias, S. G.; Bartmess, J. E.; Liebman, J. F.; Holmes, J. L.; Levin, R. D.; Mallard, W. G. *J. Phys. Chem. Ref. Data* **1988**, *17*, supplement no. 1.
(51) Nguyen, M. T.; Rademakers, J.; Martin, J. M. L. *Chem. Phys. Lett.* **1994**, *221*, 149−155.
(52) Franklin, J. L.; Dibeler, V. H.; Reese, R. M.; Krauss, M. *J. Am. Chem. Soc.* **1958**, *80*, 298−302.
(53) Nesbitt, F. L.; Marston, G.; Steif, L. J.; Wickramaaratchi, M. A.; Tao, W.; Klemm, R. B. *J. Phys. Chem.* **1991**, *95*, 7613−7617.
(54) Robin, M. B. *Higher Excited States of Polyatomic Molecules*; Academic: New York, 1975; Vol. II.
(55) Rabelais, J. W.; McDonald, J. M.; Scherr, V.; McGlynn, S. P. *Chem. Rev.* **1971**, *71*, 73−108.